

## Synthesis of Copper Oxide Nano-Rods by Microwave-Assisted Combustion Route and their Characterization Studies

Yathisha R O<sup>a</sup> and Y. Arthoba Nayaka<sup>a\*</sup>.

<sup>a</sup>Department of Chemistry, School of Chemical Sciences, Kuvempu University, Jnanasahyadri, Shankaraghatta-577 451, Karnataka, India.

Received 4 September 2017; Revised 13 October 2017; Accepted 3 November 2017

### ABSTRACT

The present study demonstrates how petal-shaped copper oxide ( $CuO$ ) nano-rod structures were fabricated using the microwave-assisted combustion method. The prepared material was annealed at a temperature of  $500^{\circ}C$  and characterized by means of optical absorption spectroscopy (UV-Vis), X-ray diffraction (XRD), Field emission scanning electron microscopy (FE-SEM), and Photo-conductivity technique (I-V characteristics). The optical energy gap of  $CuO$  nano-rods was analysed through the UV-Vis NIR spectroscopic technique and the result illustrates that the energy gap of synthesised  $CuO$  nano-rods is found to be 1.44 eV. The XRD of the synthesised sample confirms that copper oxide nano-rods are in pure monoclinic phase with lattice parameters  $x=4.675 \text{ \AA}$ ,  $y=3.343 \text{ \AA}$ ,  $z=5.183 \text{ \AA}$ . Energy dispersive analysis using X-rays confirms the existence of copper and oxygen atoms in synthesised  $CuO$  nanocrystals. FE-SEM micrographs specify that the synthesised material contains nanostructured nano-rods with a small amount of agglomeration in the product. The electrical properties of  $CuO$  film were studied through I-V characterization and the results depict that the conductance of  $CuO$  film is found to be superior under UV-light compared to in the dark.

**Keywords:** Crystalline size, Energy gap, Morphology, Petal shaped rods, Tenorite.

### 1. INTRODUCTION

Synthesis of metal-oxide and transition metal doped semiconducting nanomaterials provide opportunities for improved applications in different areas of science and technology due to their unique physical and chemical properties caused by their nano-sized dimension and large surface/volume ratio [1]. One-dimensional nanomaterial such as nano-ribbons, nano-belts, nano-cubes, and nano-prisms have become the focus of intensive research due to their distinctive properties and their significance for fabrication into high-density nanoscale devices [2]. The transition metal oxides such as copper sulphide ( $CuS$ ), cerium oxide ( $CeO_2$ ), nickel oxide ( $NiO$ ), ferrous oxide ( $Fe_2O_3$ ), and Titania ( $TiO_2$ ) are an important class of semiconductors. Among these metal-oxides, Copper (I) oxide ( $Cu_2O$ ) and copper (II) oxide ( $CuO$ ) have been gaining more popularity in recent years due to properties such as excellent thermal stability, easily available reactant materials, non-toxic, and exhibits good optical and electrical properties [3]. Due to these properties, recently most research work is mainly focused on the synthesis of different  $CuO$  nanostructures, such as nano-flowers, nano-flakes, nano-pyramid, nano-plates, and nano-bats [4].

---

\*Corresponding Author: drarthoba@yahoo.co.in

Therefore, a number of CuO nanostructures have been prepared in different morphologies by a variety of methods such as precipitation [5], solvothermal [6], hydrothermal [7], thermal evaporation [8], electrochemical [9] and combustion [10], and solid-state [11] methods. Generally, the above methods face certain drawbacks: (i) need more complicated equipment, (ii) require more additional solvent (iii) require very high temperature and pressure (iv) take more time for the reaction, and (v) more steps are required for the synthesis of CuO nanoparticles [11]. Hence to resolve the above problems, a simple and low-cost method is necessary for the preparation of CuO nanocrystals. Out of the various methods, the microwave heating process has recently become a popular and more usual process compared to other combustion methods. In this route, the microwave has got more penetrating power and it penetrates into the materials at the molecular level. This leads to the conversion of microwave energy into heat throughout the materials by either ionic conduction or dipole rotation, which results in reaction rate acceleration, yield of a homogeneous product within a few minutes, good size distribution and excellent control of stoichiometry [12]. Using this method, a number of functional materials and composites with novel structures can be obtained such as  $\alpha$ -Fe<sub>2</sub>O<sub>3</sub> nano-rings [13], NiS<sub>2</sub> nano-cubes [14], CuS nano-prisms [15], and rose-like ZnO [16] with their excellent properties.

CuO is known as a potential *P*-type semiconductor material with a narrow optical energy gap varying between 1.2- 1.4 eV [17]. When comparing CuO nanoparticles with commercially available CuO powder, the CuO nanoparticles have attracted a lot of potential applications and uses due to their nanocrystals having advanced selectivity and photo catalytic activity [18]. Due to their unconventional band structure, CuO nanoparticles have a wide range of potential applications in the fields of superconductors [19], lithium-ion batteries [20], electrochemical gas sensors [21], dye-sensitized solar cells (DSSC) [22], and electro-chemiluminescence. Therefore, it is of fundamental interest to study the structure and characterize the optical and electrical properties of high-purity, single phase CuO nanocrystals [23].

Here, we synthesised high purity CuO nano-rods using the microwave irradiation method where a solution of copper sulphate, sodium hydroxide, and urea was used. The diffraction pattern of the CuO was recorded on an X-ray diffractometer. The band gap was calculated using UV-Vis absorption studies. I-V characteristics were measured on a Keithley source meter. The rod-like structure of CuO was investigated through FE-SEM.

## 2. EXPERIMENTAL DETAILS

### 2.1 Chemicals Used

Copper sulphate pentahydrate ( $\text{Cu}(\text{SO}_4 \cdot 5\text{H}_2\text{O})$ ), sodium hydroxide ( $\text{NaOH}$ ), and Urea ( $\text{NH}_2\text{CONH}_2$ ) were procured from Himedia Laboratories Pvt. Ltd., and acetone ( $\text{CH}_3\text{COCH}_3$ ) was purchased from Merck. All chemicals were of analytical grade and were used as received without further purification. Double distilled water was used for the preparation of solutions. The synthesis of nanosized CuO rods was carried out in a domestic microwave oven (Onida power solo 17D) operating at 100% power of 700 W.

### 2.2 Synthesis of CuO Nano-Rods

To prepare CuO nanoparticles, 100 mL of 0.4 M sodium hydroxide was added drop-wise into a beaker containing 100 mL of 0.8 M copper sulphate and 0.8 M urea solution under constant stirring. When the blue-coloured homogenous reaction mixture turned into partial green, the resulting solution was kept in a microwave oven and the reaction mixture was irradiated with 60% power (175°C) of microwave energy for 15 minutes. Then, the obtained dark green precipitate of copper hydroxide was centrifuged, washed several times using distilled water,

alcohol, and acetone successively and then dried at 80°C in an oven for 5 hours. The obtained samples were calcined (500°C) in the air for 1 hour to get the desired dark brown coloured CuO nanocrystal.

### 2.3 Characterization Details

The crystallinity analysis of the nanoparticles was carried out on an X-Ray diffractometer using Cu-K $\alpha$  radiation ( $\lambda=0.15406\text{nm}$ ). The patterns were recorded in the range of 10° to 80° (2θ). The crystallite size and structure of the samples were studied using a Field emission scanning electron microscope (FESEM) fitted with an Energy-dispersive X-ray spectroscopy (EDAX) [Model: FE-SEM Carl Zeiss AG-ULTRA 55]. The absorbance of CuO nanomaterial was measured using a UV-Vis spectrophotometer (Model: USB 4000, Ocean Optics, USA). Photoconductivity properties were analysed using a Keithley low voltage source meter with the measured voltage between 0-20V [Model: Keithley 2401].

## 3. RESULTS AND DISCUSSION

### 3.1 XRD Analysis

Figure 1 shows the XRD pattern of CuO nanoparticles prepared using the microwave heating method. As can be seen in Figure 1, all diffraction peaks are assigned well to the monoclinic structure of a tenorite system. The major peaks are observed at 2θ values of 32.55°, 35.50°, 38.69°, 48.70°, 53.53°, 58.57°, 61.67°, 66.24°, 68.04°, 72.24°, 75.10° [24]. In addition, no other impurity peaks of copper hydroxide were observed in the XRD pattern, showing a single phase CuO formation, which is in agreement with JCPDS card No: 03-0884. The measured values of d-spacing and FWHM of the synthesised CuO nanocrystals are well-matched with the JCPDS card no. In addition, the peak of the XRD is broader due to the obtained materials containing a nanorange of particles. The crystalline size of the synthesised CuO nanoparticles was calculated using Scherrer's formula [25];

$$\text{Average crystalline size (D)} = \frac{0.9\lambda}{\beta \cos \theta} \quad (1)$$

where  $\lambda$  is the wavelength of CuK $\alpha$  radiation,  $\beta$  is FWHM, and  $\theta$  is Bragg's reflection angle. The average crystalline size of CuO was found to be in the range of ~21– 54 nm.

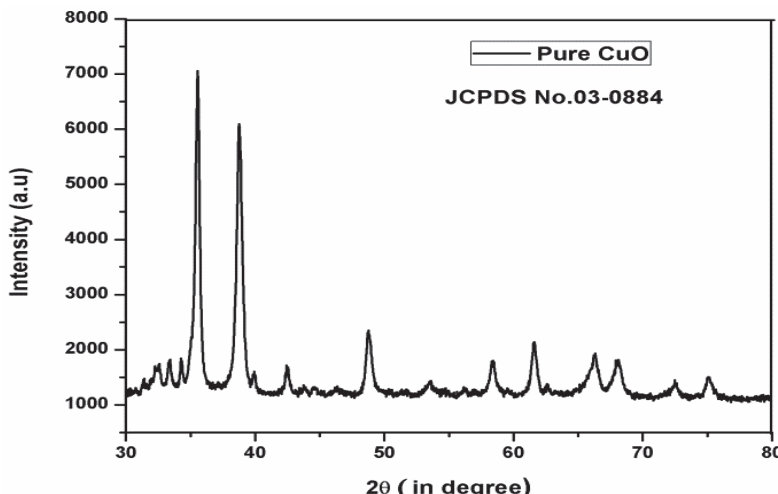


**Figure 1.** XRD pattern of petal-shaped rod-like CuO nanoparticles.

### 3.2 Structural and Elemental Analysis

Figure 2 shows FE-SEM images of synthesised pure CuO nanoparticles. The FE-SEM micrograph of samples shows that the CuO structures prepared at 60% power consist of petal-shaped rod-like CuO nanocrystals, while the low resolution ( $2 \mu\text{m}$ ) image show the minor flower-shaped particles. Particle aggregation is a major factor that controls the morphology and structure of the final product. Even though it is not yet understood, it is evident that NaOH plays an important role in the formation of the flower-like structure. Microwave irradiation has also got an influence on the surface morphology of CuO nanostructures due to its volumetric heating effect. Moreover, the vibrational frequency of the atoms during different reaction conditions plays an important role in deciding the size of the nanoparticles [26]. EDAX spectra were used to analyse the composition of CuO particles at  $500^\circ\text{C}$  and are shown in Figure 3. Based on the determination of the elemental composition of CuO nanorods (Cu=59.03% and O=40.97%), the weight percent of Cu/O ratio was found to be 1.45 and the EDAX spectrum obtained from the CuO nanoparticles shows peaks that confirm the presence of Cu and O only, which confirms that the synthesised CuO was of single phase and a high purity material. [27].

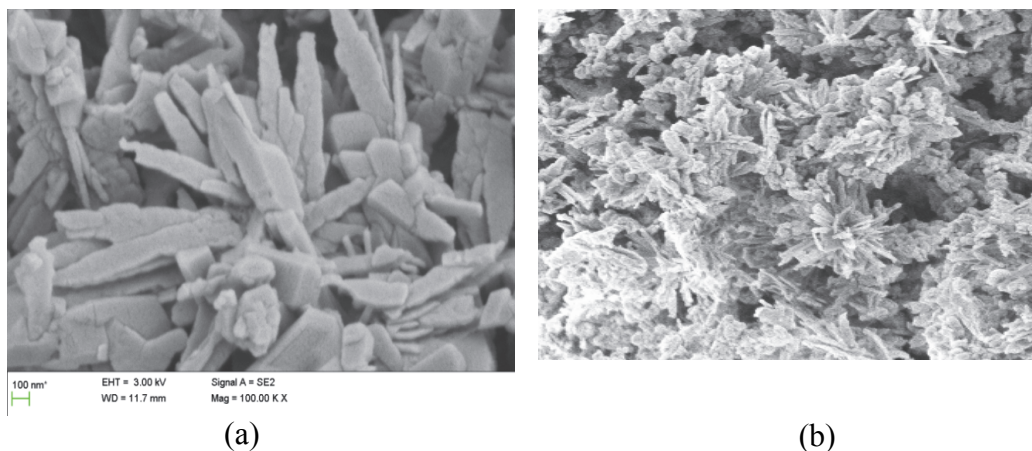


**Figure 2.** FE-SEM images of pure CuO nanoparticles (a) petal shape of rods (b) flower-like particles.

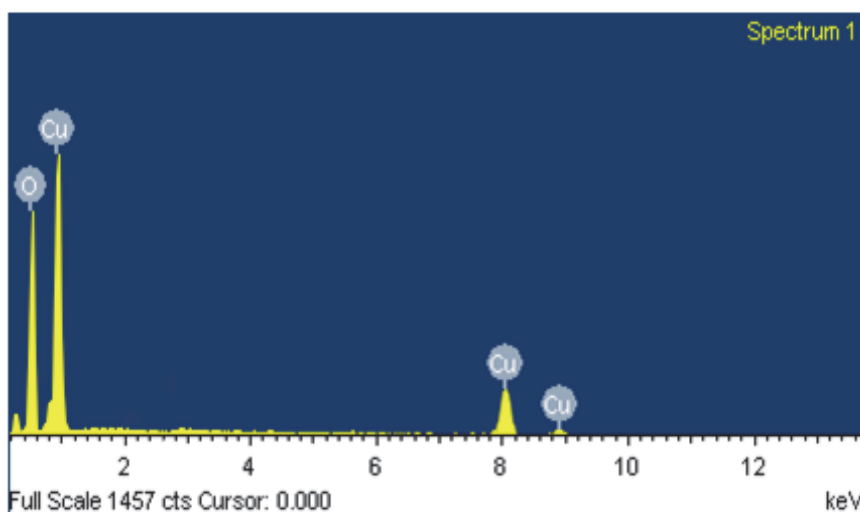


**Figure 3.** EDAX spectra of synthesised pure CuO nanoparticles.

### 3.3 UV-Visible Spectral Analysis

Figure 4 shows the optical absorption spectra of the sample annealed at 500°C temperature. A UV-Vis spectrum was measured in the range of 300 to 900nm in the wavelength region at room temperature. The measured energy gap of CuO was 1.44 eV, which was calculated from Tauc's relation,  $(\alpha h\nu)^{1/r} = B(h\nu - E_g)$  where  $h$  is the planks constant,  $B$  is a constant,  $\alpha$  is the absorption coefficient,  $v$  is the frequency of the incident radiation, and  $r$  is determined by the type of optical transition of a semiconductor. The energy band gap ( $E_g$ ) can be obtained by plotting the graph of  $(hv)$  against  $(\alpha h\nu)^{1/r}$  for various values of  $r$  and it becomes possible to determine the nature of the transitions involved. The intercepts of the straight line portion of the respective plots (at  $h\nu > E_g$ ) corresponding to zero absorption on the energy axis gives values of energy gaps [28].

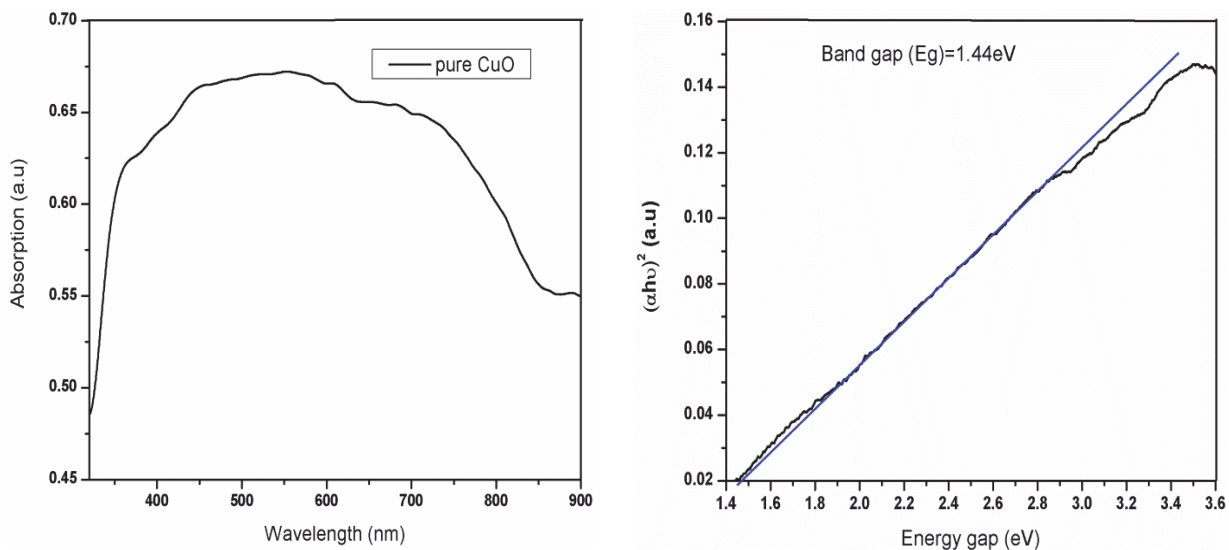


**Figure 4.** UV-Vis absorption spectra and tauc's plot of pure CuO nanoparticles.

### 3.4 I-V Characterization

The Current-Voltage (I-V) characteristics of CuO film were studied in dark as well as under light condition to check the nature of the contact between CuO and silver paste using two probe methods. The typical current-voltage curves of CuO film in dark and under light are shown in Figure 5. The area of used samples is 2x2cm<sup>2</sup>. As seen in Figure 5, the conductivity of thick CuO film was extremely small in the dark condition. It is due to the slowdown motion of electrons present in the grain boundaries. These boundaries operate as diffusion sites and impending walls, which would direct the electron movement by reducing the resistance and enhancing the conductivity. Furthermore, the improvement in conductance under the UV-light condition may be the reason for the activation of charge carriers such as electrons and also for the enhanced mobility of charge carriers [29]. Figure 5 shows the measured current of CuO films at 5V, which is 0.45A (dark condition), but the same photo-current was also observed at low voltage (4V) in the UV-light condition. The measured optical energy gap, conductivity, and resistivity are very valuable for the application of fabrication of optical devices [30].

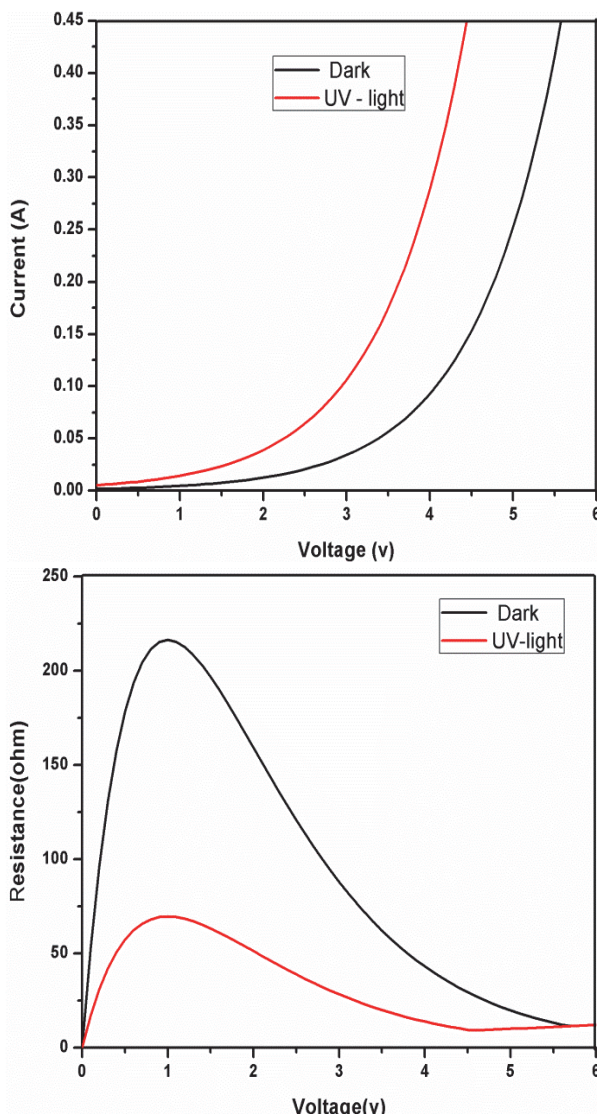


**Figure 5.** I-V characteristics of CuO nanoparticles under dark as well as UV-light conditions.

#### 4. CONCLUSIONS

In summary, rod-like CuO nanoparticles with monoclinic structure were synthesised using the microwave combustion method with urea used as fuel. XRD studies show that the synthesised CuO nanoparticles are of monoclinic structure; it also show the average size of the particles. A FESEM observation displays the surface morphology of rod-shaped CuO particles in the nanometer dimension. UV-Vis spectra show that the optical band gap of CuO is 1.45eV, which is calculated from Tauc's relation. I-V indicates the photo-current conversion efficiency of CuO nanoparticles.

#### ACKNOWLEDGEMENTS

The Authors would like to thank the Science and Engineering research board (SERB), Delhi for providing financial support to carry out this research work. The authors are also thankful to the Indian Institute of Science (IISC), Bangalore for providing XRD and SEM facilities.

## REFERENCES

- [1] D. Laha, A. Pramanik, A. Laskar *et al.*, Materials Research Bulletin **59** (2014) 185.
- [2] Y. Ping Que, J. Weng, L.H. Hu, J. Huai Wu *et al.*, Journal of Power Sources **307** (2016) 138.
- [3] X. Fuku, K. Kaviyarasu, M. Matinise *et al.*, Nanoscale Research Letters **11/386** (2016) 10.
- [4] K. Outokesh, M. Hosseinpour *et al.*, Industrial and Engineering Chemistry Research **50** (2011) 3545.
- [5] T. Wang *et al.*, Materials Chemistry and Physics **139** (2013) 605.
- [6] L. Li, D. Mao, J. Yu *et al.*, Journal of Powder Source **279** (2015) 404.
- [7] A.D. Khalaji, K. Jafari *et al.*, Journal of Nanostructures **2** (2013) 508.
- [8] S. Sonia, N.D. Jayram, P.S. Kumar *et al.*, Super lattice and Microstructure **66** (2014) 8.
- [9] I.S. Yahia, A.A.M. Farag *et al.*, Optik-International journal for light and electron optics **127** (2016) 1429.
- [10] N.C.S. Selvam, R.T. Kumar *et al.*, Power Technology **211** (2011) 255.
- [11] S. Jing, W. Wang, Q. Yue *et al.*, Applied Energy **175** (2016) 141.
- [12] V. Eskizeybek, A. Avci *et al.*, Crystal Research & Technology **46** (2011) 1100.
- [13] X. Hu, J. C. Yu, J. Gong *et al.*, Advanced Materials **19** (2007) 2324.
- [14] H. Pang, C. We, X. Li *et al.*, Scientific Reports **4** (2014) 3577.
- [15] S. W. Hsu, C. Ngo, A. R. Tao *et al.*, Chemistry of Materials **27** (2015) 4957.
- [16] T. Jiang, Y. Wang *et al.*, Applied Surface Science **311** (2014) 608.
- [17] R. Behera *et al.*, Researcher **4**, 12 (2012) 29.
- [18] A.P. Moura, L.S. Cavalcante *et al.*, Advanced Powder Technology **21** (2010) 202.
- [19] F.Teng, W. Yao *et al.*, Sensors and Actuators B **134** (2008) 768.
- [20] P. Subalakshmi *et al.*, Journal of Alloys and Compounds **690** (2017) 523.
- [21] A.Umar, A.A.Alshahrani *et al.*, Sensors and Actuators B: Chemical **250** (2017) 24.
- [22] H. Kidowaki, T. Oku, T. Akiyama *et al.*, Journal of Materials Science Research **1/1** (2012) 138.
- [23] Z. Yan, Z. Xu, J. Yu, G. Liu *et al.*, Electroanalysis **26** (2014) 2017.
- [24] C.C. Vidyasagar, Y. A. Naik , *et al.*, Powder Technology **214** (2011) 343.
- [25] L. Xu, H.Y.Xu, F. Wang *et al.*, Journal Korean Ceramics Society **49/2** (2012)151.
- [26] M. Vaseem, A. Umar *et al.*, Journal of Physical Chemistry C **112** (2008) 5729.
- [27] S. Muthukumaran *et al.*, Optical Materials **34** (2012) 1953.
- [28] Y. Wang, T. Jiang, *et al.*, Applied Surface Science **355** (2015) 196.
- [29] R.O. Yathisha, Y. Arthoba Nayaka *et al.*, Materials Chemistry and Physics **181** (2016) 175.
- [30] S. Illican, Y. Caglar *et al.*, Journal of Optoelectronics and Advanced Materials, **10/10** (2008) 2578.

